Heliospheric Current Sheet Probe

Yu Yi

Laboratory for Atmospheric and Space Physics, University of Colorado, Boulder, CO 80309, USA

(Manuscript received 15 November 1995)

Abstract

Space explorations by spacecraft have detected the solar wind and the interplanetary magnetic field (IMF), whose existences had been suggested to explain the narrow comet plasma tail formation before the space age. Thereafter, a global magnetic structure seperating the opposite polarity regions of IMF in the heliosphere was discovered (Wilcox and Ness, 1965). It is called heliospheric current sheet (HCS). Comets have been proved as the useful heliospheric probes. Recently, another capability of comet as a probe of HCS was suggested by Yi (1994). In the process of comet plasma tail disconnection events (DEs) showing the ray folding and main tail severance between the folding rays (Brandt, 1982), the folding rays preceding DE might be the visualization of HCS draped around comet, In order to test this new idea, the association of comet Halley 16 DEs with comet crossings of HCS confirmed by spacecraft observations at the time of comet Halley apparition 1985~1986 was investigated.

1. Introduction

Heliospheric Current Sheet

In an idealized case, the sun's magnetic field could consists of two magnetic hemispheres of radial field lines of opposite polarity in each hemisphere. In one hemisphere, all the field lines would be pointing away from the sun, while they would all point toward the sun in the other. At the boundary between the two hemispheres, there would be a planar current sheet separating the two regions of opposite polarity.

In reality, this current sheet is not strictly planar, but has a slowly undulating surface that spirals out from the sun. An object in orbit about the sun may periodically pass through this current sheet moving from the region of outward-pointing magnetic field to the inward-pointing hemisphere. This gives the appearance of magnetic 'sectors' in the IMF, some containing fields pointing sunward, others pointing anti-sunward. This sector structure in Figure 1 was discovered in 1965 in data from the IMP-1 satellite (Wilcox and Ness, 1965).

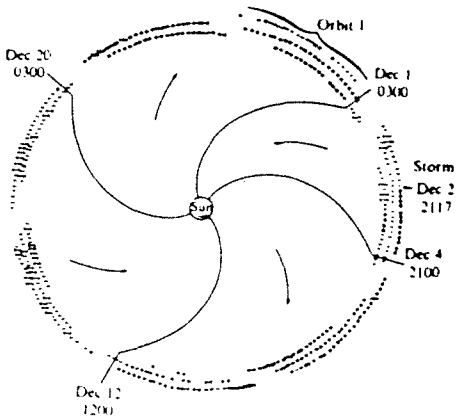

Fig. 1. The Heliospheric sector structure of the interplanetary magnetic field observed by the IMP-1 satellite. The plus polarity means the field directed out of the sun and the minus corresponds to the field toward the sun (Wilcox and Ness, 1965).

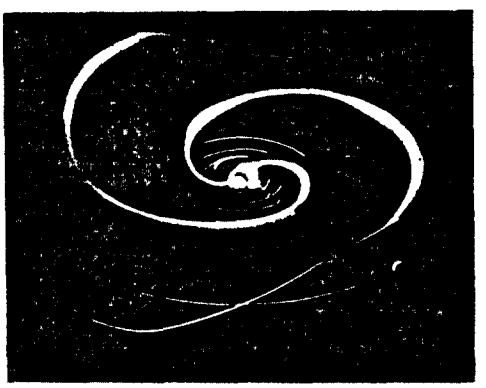

Fig. 2. An illustration of the heliospheric current sheet. By permission of Hoeksema.

Figure 2 shows illustration of the 3-dimensional warped heliospheric current sheet (HCS), which gives this sector structure observed near the ecliptic plane. These undulations can reach moderately high solar latitudes (50° or more during periods of high solar activity (Hoeksema, 1989)). During solar minimum the HCS reaches about 20° from the heliospheric equator.

In addition to a reversal of the magnetic field polarity, the solar wind magnetic field magnitude, flow speed, density, and temperature also show longitudinal variations within a sector. The typical variations of those parameters within a two-seventh sector of the 27-day corotation period, which rotates past the Earth in $\frac{2}{7} \times 27$ days $= 7\frac{3}{4}$ days, are as follows (Wilcox and Ness 1965) : the magnitude of the IMF ($|B|$) and the flow speed (w) rise steeply from the low pre-boundary levels to maximum values over a period of about two days, then gradually decline back to their previous level over the next several days. The geomagnetic index $\sum Kp$ (daily sum) varies synchronously with the flow speed. The density (N_e) also rises sharply at the edge of the boundary, then quickly falls into a slightly depressed value for a couple of days, followed by another density increase. The plasma temperature (T) behaves much like the flow speed, quickly rising and then gradually falling back to its fiducial level.

Potential Field Model of HCS

The location of the HCS can be predicted using a potential field - source surface model of the coronal magnetic field based on photospheric magnetic field observations. At the source surface, all magnetic field lines are assumed to be frozen in the plasma and are carried radially outward into the heliosphere by the solar wind. By this assumption the neutral line on the coronal source surface maps radially outward to form the HCS. There are some disadvantages to this approach, but for large-scale phenomena it is sufficient. This IMF structure of the HCS when projected to 1 AU is in reasonable agreement with the observations (Hoeksema, 1989).

2. Spacecraft Observations of HCS

Note that neutral line calculations are available for different source surfaces. Here we consider coronal source surface radii of 1.6 R_{SUN}, 2.0 R_{SUN}, and 2.5 R_{SUN}. The farther the coronal source surface is located from the solar surface, the less structure the current sheet exhibits. Specifically, as the

coronal source surface radius increases, the HCS remains closer to the projected solar equator for all Carrington longitudes. The HCS model dependency on the coronal source surface radius is shown in Figure 3, Where the curves for 2.0 R_{SUN}, 2.5 R_{SUN} are plotted.

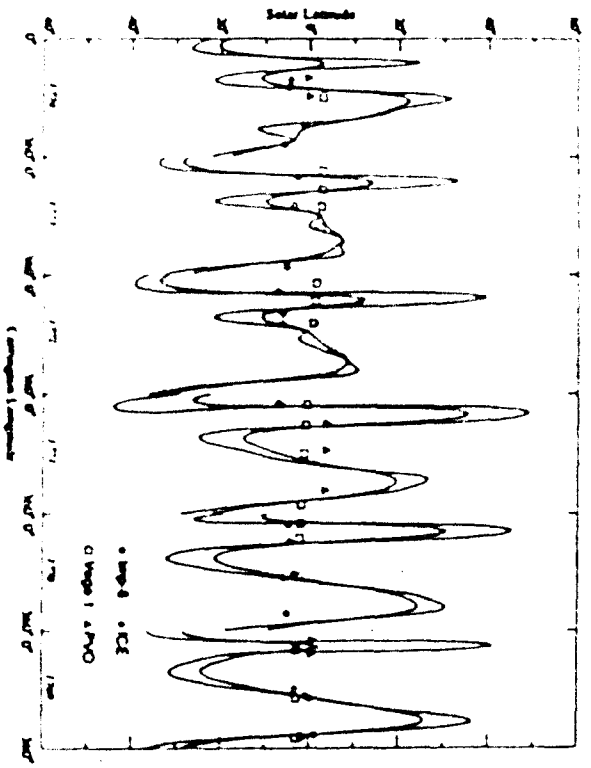

Fig. 3. HCS fit to spacecraft data. Displayed are the four spacecraft (IMP-8, ICE, PVO, and Vaga-1) detections of the HCS and the HCS positions for source surface radii 2.0 R_{SUN} and 2.5 R_{SUN}. For clarity we have left off the 1.6 R_{SUN} source surface. The 2.5 R_{SUN} source surface can be identified as the curve typically closer to the solar equatorial plane.

For each of the four spacecrafs (IMP-8, PVO, ICE, Vega-1) we obtained the positions of the HCS crossing on the heliospheric source surface via corotation. Then we calculated the rms distance of the spacecraft from the HCS for each coronal source surface radius (1.6 R_{SUN}, 2.0 R_{SUN} and 2.5 R_{SUN}) for Carrington rotations 1769 to 1774. The coronal source surface at 2.5 R_{SUN}, fit the spacecraft data best for Carrington rotations 1770 through 1774, while the coronal source surface at 2.0 R_{SUN} produced the lowest *rms* values for Carrington rotation 1769. However, in Carrington rotation 1769, the difference between the *rms* values for coronal source surfaces of 2.0 R_{SUN} and 2.5 R_{SUN} was small. For all subsequent results quoted in this paper, we will use coronal source surface 2.5 R_{SUN} for Carrington rotations 1770-1774. Figure 3 shows the HCS positions observed by spacecraft compared with the projected current sheets for 2.0 R_{SUN} and 2.5 R_{SUN}. The best-fit HCS is shown in Figure 4.

For Carrington rotations 1769~1774, the four spacecrafts crossed the sector boundaries a total of 48 times. The mean angular deviation between the spacecraft's measurement of the HCS and the position given by the extrapolated potential field model was 6.7°, while the *rms* dispersion was 8.9°. However, nearly 13% of the *rms* residual was produced by the Vega-1 detection of the HCS on 1986 March 17.7. If we neglect this crossing, the *rms* dispersion drops to 7.8°, while the mean deviation decreases to 6.2°.

3. Associations of Comet Halley DEs with HCS Crossings

Comet Halley passed through this current sheet many times in 1985~1986, coinciding with many of the observed DEs. The 16 DEs were reported during this period (Yi et al. 1994). These DEs are overplotted on the best-fit HCS in Figure 4. Due to the retrograde motion of comet Halley, it detects one extra Carrington rotation than the Earth does. To model this we duplicated CR 1771. Since there were no DEs observed in this duplication period, the addition does not affect the

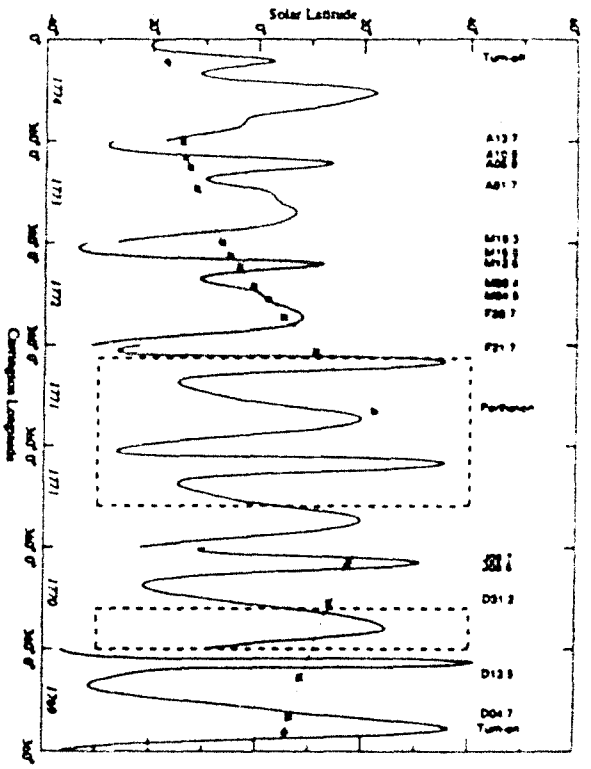

Fig. 4. Comparison of comet Halley's 16 DEs to the best-fit HCS. The solid curve depicts the 'best fit' current sheet as determined by the spacecraft data. The light-dashed curve represents comet Halley's orbit with each individual DE denoted by an asterisk. Ion tail turn-on/off and perihelion are marked by diamonds and a triangle, respectively. The heavy dashed boxes correspond to periods with few or no observations of comet Halley. Due to the retrograde motion of comet Halley, we duplicated CR 1771.

The association of DEs with sector boundaries seems clear. There is almost a one to one correspondence between HCS crossings and DEs, i.e., the number of opportunities for DE production at crossings is approximately equal to the observed number of DEs during this time interval. Recall that this analysis is restricted to those DEs shown by wide-field images in *The international Halley Watch Atlas of Large-Scale Phenomena*(Brandt, et at., 1992).

Where there are gaps, they are consistent with the observing conditions. An excellent indicator of possible coverage is the histogram of images used in *The International Halley Watch Atlas of Large-Scale Phenomena*. Specifically, the coverage in late December 1985 and around perihelion (9 February 1986) is quite sparse. DEs that would be expected in these time periods probably were not observed.

We find a mean deviation between the DEs' positions and the HCS of 11.3° and an *rms* value of 14.7°. The magnetic reconnection between the anti-parallel magnetic field lines draped around the comet ionosphere occurs over a period of time. Therefore, there should be a time delay between the comet encountering the HCS and the observation of a DE for the sunward reconnection model. Niedner and Brandt (1978) estimated ~ 0.7 day. To account for this delay, we shifted each DE position an equal amount and found which shift produced the lowest *rms* dispersion. The lowest *rms* dispersion was 13.5° and occurred approximately at a 1 day shift.

The point of minimum distance to the HCS may not be the actual place where the comet crossed the HCS. To consider this case, we calculated the distance between the DE and the position on the HCS with the same(or approximately the same) heliospheric latitude as the DE. For no shift, the *rms* value was 19.2°. The minimum, 18.9°, occurred at approximately a 0.25~day shift of DE position. The difference between the best *rms* value of the shifted DE positions to that of no shift is only 0.3°. Hence, we do not believe this case can permit an accurate determination of the actual time between the comet penetration of the current sheet and the first

visible onset of the DE. For consistency, we chose a 1-day shift of the DE positions, which produced an *rms* dispersion of 20.2° for this case.

To test quantitatively whether DEs are associated with sector boundaries, we ran 5,000 cases of 16 DEs randomly placed on comet Halley's orbit for the time period between plasma tail turn-on and turn-off. There were two long periods where there were little or no observations. For calculating the random positions corresponding to the observation periods along comet Halley's orbit, we did not permit random positions in the observation periods of 1985 Dec. 20~30 and 1986 Jan. 20-Feb. 20.

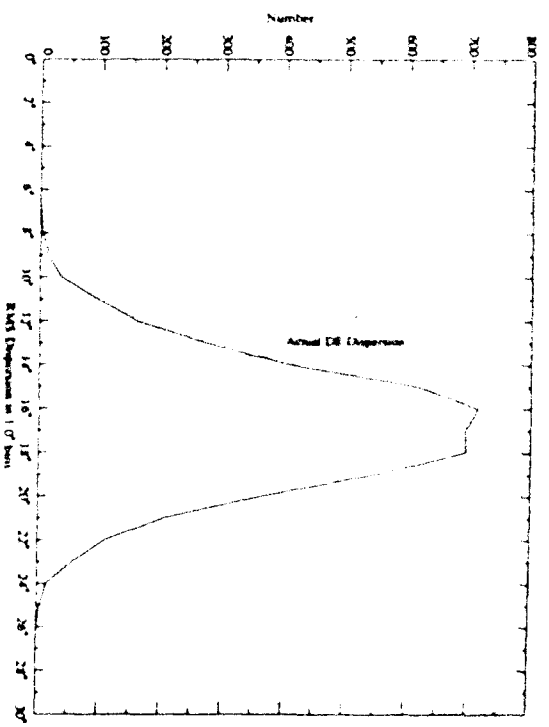

Fig. 5. Plots in 1.0° bins of the *rms* dispersion of 5000 iterations of 16 DEs randomly placed along comet Halley's orbit as described in the text. The *rms* dispersion is for the case where we calculated the minimum distance between the HCS and the DE. The dashed line is the actual *rms* dispersion (13.5) of comet Halley's 16 DEs calculated this way and shifted by approximately one day.

When we calculated the minimum distance to the HCS with no latitude restriction, we obtained an *rms* value of 17.3°. Of these 5,000 iterations 90.9% were greater than the 13.5° which resulted from shifting the data by one day while 83.3% were greater than the 14.7° obtained from no shift. The statistics of this case is shown in Figure 5.

Quantitatively, the dispersion of the total samples around the best-fit HCS is 8.9° for the 48 spacecraft determination and 13.5° for the 16 DEs. When the two worst cases are removed, the dispersions are 7.2° for spacecraft determinations and 10.0° for DEs. When the four worst cases are out, the dispersions are 6.4° for spacecraft determinations and 8.7° for DEs.

4. Conclusions

The comet plasma observations have predicted many heliospheric properties such as the continuous corpuscular stream (Biermann, 1951), called the solar wind, the interplanetary magnetic field (IMF) (Alfvén, 1957) frozen in the solar wind, and the high speed stream in high solar latitudes. Recently Yi (1994) simulated the influence of HCS crossing on comet plasma tail. It was shown that the comet plasma tail disconnection events (DEs), whose morphological evolution showing the ray folding and main tail severance between the folding ray (Brandt, 1982), happened when a comet crossed a HCS. In that process, the folding rays were suggested as the visualization of HCS crossed by comet.

In order to confirm the simulation, the DEs of comet Halley were chosen to look for the correlation between DEs and comet's HCS crossings. The comet Halley interval was a good one in many respects, with intensive imaging from the ground, good HCS data, and

solar wind data available from many spacecrafts. The best-fit HCS is determined by comparing different models to the spacecraft detections of HCS crossings. Finally, the 16 DEs observed in comet Halley were compared to best-fit HCS. Comparison of the solar wind conditions and 16 DEs in Halley's comet shows that DEs are associated primarily with crossings of the HCS. DEs are not apparently associated with any other properties of the solar wind, such as high speed streams and the dynamic pressure increase of solar wind (Yi et al., 1994).

The on-going Ulysses mission will be another good chance to test the high-latitudinal variations of the HCS and its relationship with cometary DEs. During the times of the Ulysses mission, we can gather cometary images, and correlate the cometary data with solar wind conditions as measured by Ulysses. Future comet rendezvous mission would be in situ observation test of DE mechanism.

Acknowledgments. I thank solar wind data centers such as NSSDC for IMP-8 and ICE data, and UCLA for PVO data, and Dr. Todd Hoeksema at Wilcox solar Observatory for the HCS data.

References

Alfvén, H., On the Theory of Comet Tails, Tellus, 9, 92~96, 1957.

Biermann, L., Kometenschweife und Solar Korpuskularstrohlung, Zs. F. Astrophys., 29, 279-286, 1951.

Brandt, J.C., Observations and Dynamics of plasma tails, in Comets, ed. L.L. Wilkening, University of Arizona, Tucson, p.519, 1982.

Brandt, J.C., Niedner, M.B., Jr., Rahe, J., in The International Hally watch Atlas of Large-Scale Phenomena, LASP, U. of Colorado, Boulder, 1992

Hoeksema, J.T., Extending the Sun's Magnetic Field through the Three-Dimensional Heliosphere, Adv. Space Res., 9, (4)141-152, 1989.

Niedner, M.B., Jr. and Brandt, J.C., Interplanetary Gas. XXIII. Plasma Tail Disconnection Events in Comets : Evidence for Magnetic Field Line Reconnection at Interplanetary Sector Boundaries?, Astrophys. J., 223, 655, 1978.

Wilcox, J.M. and Ness, N.F., Quasi-stationary corotating structure in the interplanetary medium, J.Geophys. Res., 70, 5793, 1965.

Yi, Y. Global Magnetohydrodynamic simulation of a Comet : When a Comet Crosses a Heliospheric Sector Boundary, Korean J. Geophys. Res., 22, 6~23, 1994.

Yi, Y., F.M. Caputo, and J.C. Brandt, Disconnection Events (DEs) and Sector Boundaries : The Evidence from Comet Halley 1985~1986, Planet. Space Sci., 42, 705~720, 1994.